2-(Benzimidazol-2-yl)quinoxalines: A Novel Class of Selective Antagonists at Human A_1 and A_3 Adenosine Receptors Designed by 3D Database Searching

Ettore Novellino,*,[†] Barbara Cosimelli,[†] Marina Ehlardo,[†] Giovanni Greco,[†] Manuela Iadanza,[†] Antonio Lavecchia,[†] Maria Grazia Rimoli,[†] Annalisa Sala,[†] Antonio Da Settimo,[‡,⊥] Giampaolo Primofiore,[‡] Federico Da Settimo,[‡] Sabrina Taliani,[‡] Concettina La Motta,[‡] Karl-Norbert Klotz,[§] Daniela Tuscano,[‖] Maria Letizia Trincavelli,[‖] and Claudia Martini[‖]

Dipartimento di Chimica Farmaceutica e Tossicologica, Università di Napoli "Federico II", Via D. Montesano, 49, 80131 Napoli, Italy, Dipartimento di Scienze Farmaceutiche, Università di Pisa, Via Bonanno 6, 56126 Pisa, Italy, Institut für Pharmakologie und Toxikologie, Universität Würzburg, Versbacher Strasse 9, 97078 Würzburg, Germany, and Dipartimento di Psichiatria, Neurobiologia, Farmacologia e Biotecnologie, Università di Pisa, Via Bonanno 6, 56126 Pisa, Italy

Received August 10, 2005

The Cambridge Structural Database (CSD) was searched through two 3D queries based on substructures shared by well-known antagonists at the A_1 and A_3 adenosine receptors (ARs). Among the resulting 557 hits found in the CSD, we selected five compounds to purchase, synthesize, or translate synthetically into analogues better tailored to interact with the biological targets. Binding experiments using human ARs showed that four out of five tested compounds turned out to be antagonists at the A_1AR or A_3AR with K_i values between 50 and 440 nM. Lead optimizations of 2-(benzimidazol-2-yl)quinoxalines (BIQs, **3**) gave the best results in terms of potency and selectivity at the A_1 and A_3 ARs. Particularly, 2-(4-ethylthiobenzimidazol-2-yl)quinoxaline (**3e**) exhibited K_i values at the A_1AR, $A_{2A}AR$, and A_3AR of 0.5, 3440, and 955 nM, respectively, whereas 2-(4-methylbenzimidazol-2-yl)quinoxaline (**3b**) displayed at the same ARs K_i values of 8000, 833, and 26 nM, respectively.

Introduction

Adenosine is an endogenous signaling nucleoside released from most cells that is responsible for many physiological processes.[1−5] Once in the extracellular space, it modifies cell functioning by triggering specific cell membrane G-protein-coupled receptors that modulate several effector systems, including adenylate cyclase, potassium and calcium channels, phospholipase C or D, and guanylate cyclase. At least four adenosine receptor (AR) subtypes, classified as A_1, A_2 (A_{2A}, A_{2B}), and A_3, have been identified as mediators of these effects.[6] Each receptor subtype has been indicated as a target for the development of agonist- and antagonist-based therapies against a wide range of pathologies (CNS disorders, cardiac arrhythmia, ischemic injuries, asthma, renal failure, and inflammatory diseases).

In particular, the A_1AR is extensively expressed in both the CNS and peripheral tissues, such as kidney, lung, bladder, adipose tissue, and heart.[6] The main potential therapeutic applications of A_1AR antagonists are for the treatment of cognitive deficits, CNS disorders such as Alzheimer's disease, renal failure, cardiac bradiarrhythmias, and asystolic arrest.[2,7]

The $A_{2A}AR$ is highly coexpressed with the dopamine D_2 receptor in the striatum of the basal ganglia, where an antagonistic cross-talk between $A_{2A}AR$ and D_2 has been reported.[8−10] Consequently, potent and selective $A_{2A}AR$ antagonists are currently investigated as new drugs for the treatment of neurodegenerative disorders, such as Parkinson's disease.[11,12]

The A_3AR is widely distributed in peripheral organs with the largest expression detected in the testis, liver, and lung, but it is also expressed in the CNS and heart.[13] A_3AR antagonists might be therapeutically useful for the acute treatment of stroke, for glaucoma, and also as antiasthmatic and antiinflammatory drugs.[14−16]

In this scenario, the search for novel potent and selective antagonists at the different ARs is still an attractive field of research.

In recent years, it has been shown that database searching is a valuable tool to discover novel lead compounds.[17] The input for the search engine can be a query made up of a substructure (two-dimensional (2D) search). When the query includes torsion angles and/or interatomic distances, the search is of three-dimensional (3D) type. Queries are typically built up from a pharmacophore model or from the structure of a highly active compound whose target-bound conformation is known from X-ray or NMR experiments or is the only one energetically allowed. A database search ends up yielding a number of hits (i.e., structures matching the query) between zero and thousands. If the number of hits is too small or too large, the search is repeated, adjusting the settings of the query until a manageable number of hits is found. Typically, the user focuses the search on "drug-like" structures[18] by applying filters on the basis of molecular weight, the number of heteroatoms, calculated lipophilicity, the number of rotatable bonds, and any other suitable physicochemical parameter. Because hits may not be tailored to interact with the target biomacromolecule (e.g., because they are exceedingly bulky, hydrophilic, etc.) or are chemically unstable, their

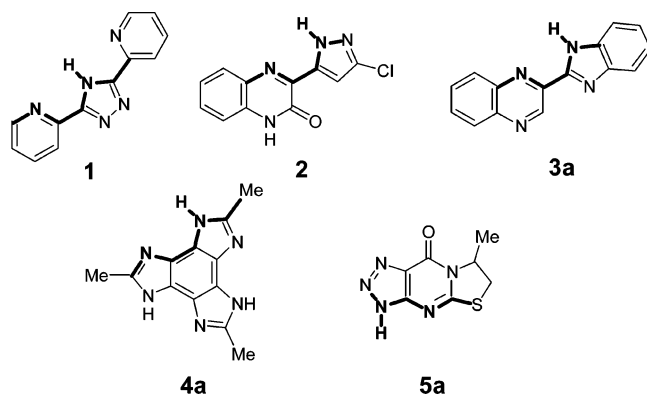* To whom correspondence should be addressed. Phone: (+39)-081678644. Fax: (+39)081678630. E-mail: novellin@unina.it.
† Università "Federico II" di Napoli.
‡ Dipartimento di Scienze Farmaceutiche, Università di Pisa.
§ Universität Würzburg.
‖ Dipartimento di Psichiatria, Neurobiologia, Farmacologia e Biotecnologie, Università di Pisa.
⊥ In memory of Prof. Antonio Da Settimo, who died in February 2005.

Table 1. Affinities at Human A_1, A_{2A}, and A_3 ARs of Compounds Designed as A_1AR and/or A_3AR Antagonists by 3D Database Searching

cmpd	K_i (nM)[a]		
	hA_1[b]	hA_{2A}[c]	hA_3[d]
1	>10000	>10000	>1000
2	3336 ± 557	>10000	125 ± 20
3a	50 ± 15	561 ± 17	763 ± 13
4a	>10000	>10000	130 ± 3
5a[e]	>10000	>10000	440 ± 33
DPCPX	0.5 ± 0.03	337 ± 28	>1000
NECA	14 ± 4	16 ± 3	73 ± 5
Cl-IBMECA	890 ± 61	401 ± 25	0.22 ± 0.02

[a] The K_i values are means ± SEM of at least three determinations derived from an iterative curve-fitting procedure (Prism program, GraphPad, San Diego, CA). [b] Displacement of specific [³H]DPCPX binding in membranes obtained from hA_1AR stably expressed in CHO cells. [c] Displacement of specific [³H]NECA binding in membranes obtained from $hA_{2A}AR$ stably expressed in CHO cells. [d] Displacement of specific [¹²⁵I]AB-MECA binding in membranes obtained from hA_3AR stably expressed in CHO cells. [e] Assayed with a purity degree of 96%.

structure is often converted into derivatives with more chances of displaying the desired biological properties. Several examples of 3D database searches aimed at identifying new leads are documented in literature.[17,19–24]

We applied the 3D database searching approach to design new antagonists at the A_1 and A_3 ARs. The Cambridge Structural Database (CSD)[25] (version 5.25, November 2003) was scanned using two different queries, each made up of a pharmacophore substructure whose 3D disposition was defined by torsion angles. Our working hypothesis was that pharmacophoric features of A_1-AR and A_3AR antagonists could be found in some of the structures deposited in the CSD that have never been assayed or even considered for such biological properties. Among the resulting 557 hits, we selected five compounds to purchase, synthesize, or translate synthetically into analogues thought to be more suited for binding to the target receptors. Four compounds turned out to be active as antagonists at the human A_1AR or A_3-AR with K_i values between 50 and 440 nM (Table 1). Among these compounds, 2-(benzimidazol-2-yl)quinoxaline (BIQ), labeled as **3a** in this contribution, was selected as the most promising lead to optimize affinity and selectivity at both the A_1AR and the A_3AR. In a few make-and-test cycles, we obtained two BIQ derivatives active as selective antagonists at the A_1AR (**3e** with K_i = 0.5 nM) and A_3AR (**3b** with K_i = 26 nM) (Table 4).

3D Database Search and Lead Design

The six highly potent selective antagonists at the A_1-AR and A_3AR reported in Figure 1 contain one of the following substructures: (1) C–N–C–C–NH–C (extracted from the A_1AR antagonists **I**[26] and **II**[27] as well from the A_3AR antagonist **IV**[28]) or (2) C–C–N–C–NH–C (featured by the A_1AR antagonist **III**[29] as well as by the A_3AR antagonists **V**[30] and **VI**[31]). The two substructures were further detailed through 2D constraints based on connectivity and 3D constraints based on torsion angles to yield the queries used to scan the CSD[32] (Figure 2). The whole process of lead finding is illustrated in Figure 3. The searches performed with queries 1 and 2 gave 299 and 258 hits, respectively. Each hit was subsequently inspected on the basis of "drug-likeliness" criteria proposed by Lipinski,[18] chemical stability, and ease of synthesis. At the end of this step, we selected five structures filed in the CSD with the reference codes *bzquxl*,[33] *biyroq*,[34] *fapwoi*,[35] *hexpab*,[36] and *sortey*.[37] *Biyroq* (**1**) was purchased from ChemBridge Corp. (San Diego, CA); *hexpab* (**2**) was prepared as described in the literature.[36] The remaining three hits (*bzquxl*, *fapwoi*, and *sortey*) were synthetically translated into analogues expected to display higher affinity as antagonists at the A_1AR and/or A_3AR, namely compounds **3a**, **4a** (less bulky), and **5a** (less hydrophilic).

Chemistry

Compounds **3a–o** were prepared by following the published synthetic procedure (Schemes 1 and 2) for the obtainment of **3a**.[38] In brief, the starting quinoxaline-2-carboxylic acid **6** was heated in polyphosphoric acid with the appropriate phenylendiamine **7a–o** to obtain the target benzimidazolequinoxaline **3a–o**.

The *o*-phenylendiamines **7** were all commercially available, except **7d** and **e**; their synthesis involved the preparation of **10e**, in accordance with the published procedure for **10d**,[39] followed by a simple reduction of the nitro group to an amino (Scheme 3).

Compound **4a** was prepared starting from the commercially available **11** (Ambinter, Paris, France) and acetic anhydride.[40] Product **4d**, previously reported to
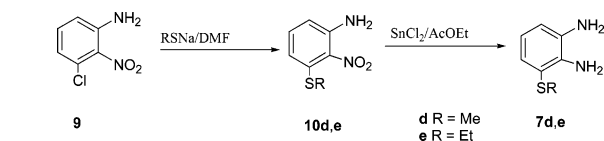
Scheme 1
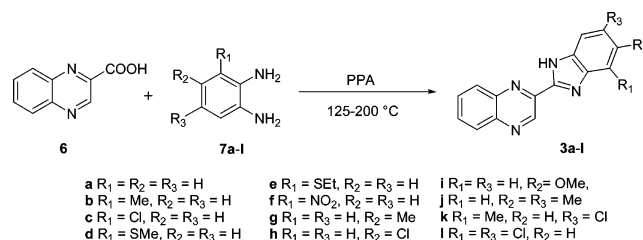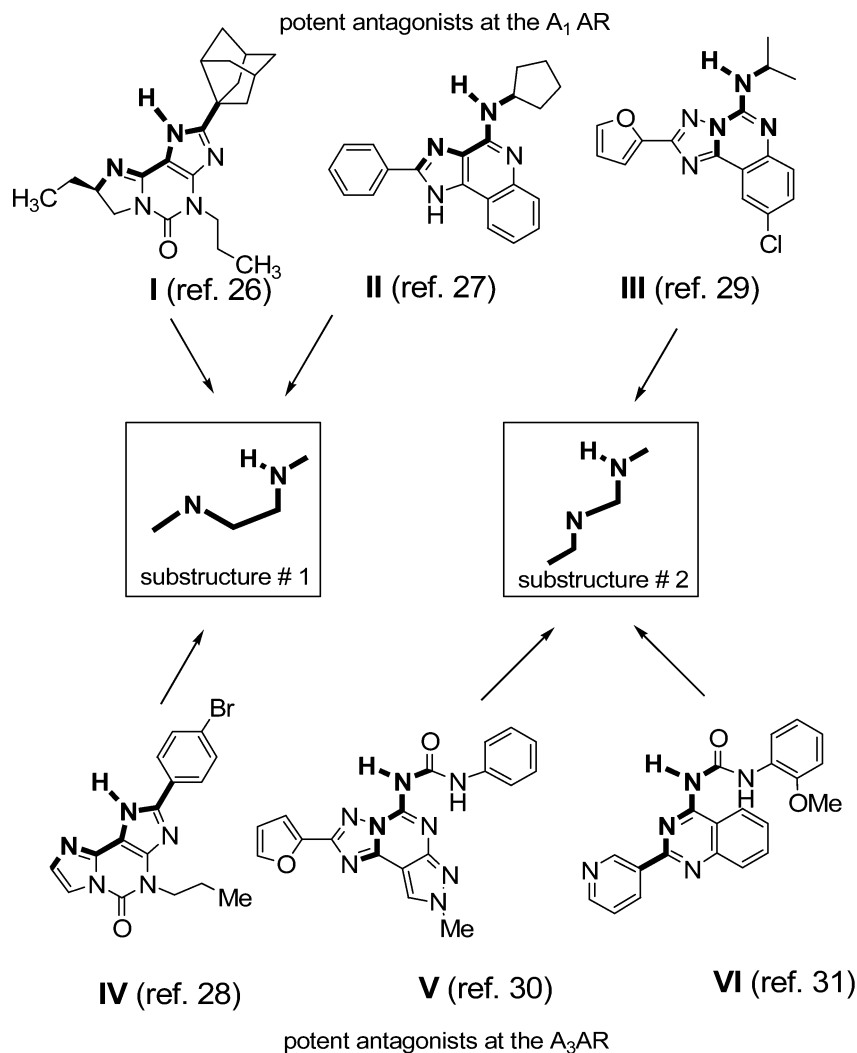

Scheme 2
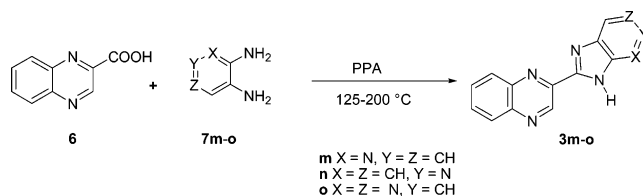
Scheme 3

Figure 1. Substructures extracted by potent antagonists at the A₁AR and A₃AR.
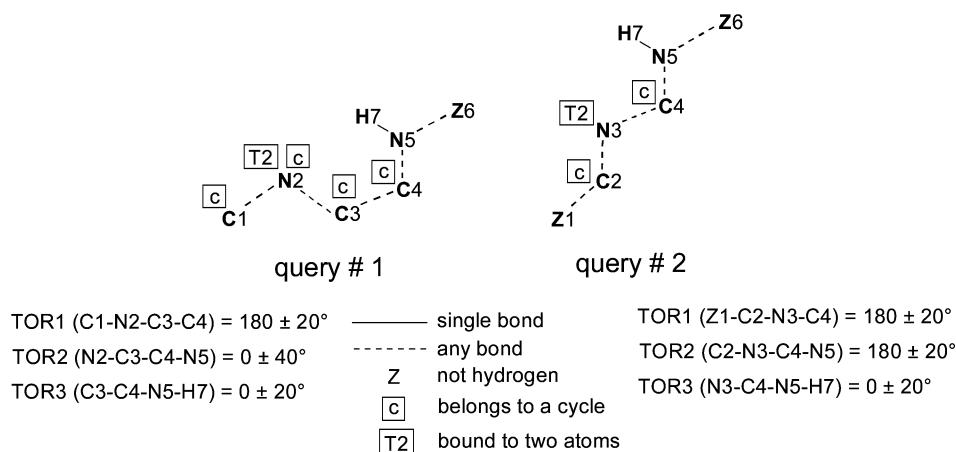

Figure 2. Two 3D queries employed to search the CSD using the ConQuest search engine.[32] Organometallic compounds were excluded from the search by the "only organics" option. The ranges of the torsion angles were chosen to yield a manageable numbers of hits.

be obtained by reaction of **11** and propionic acid with a low yield (2.6%),[35] was prepared from **11** and propionic anhydride with satisfactory yields (34%). The unknown **4b,c** were synthesized, together with derivatives **4a,d**, by the reaction of **11** with a mixture of acetic anhydride and propionic anhydride in a large excess (Scheme 4).

The known compounds **5b,c** were obtained following a reported procedure;[41] product **5d** was similarly syn-

thesized, reacting the diamino derivative **12** and 1,2-dichloroethylene in alkaline medium to give **13**, which was successively cyclized to the target triazole (Scheme 5).

Finally, compound **5a** was obtained with a very small yield, following a different synthetic strategy, reported in Scheme 6; many other attempts at preparation failed. The known compound **14**[42] was allowed to react with
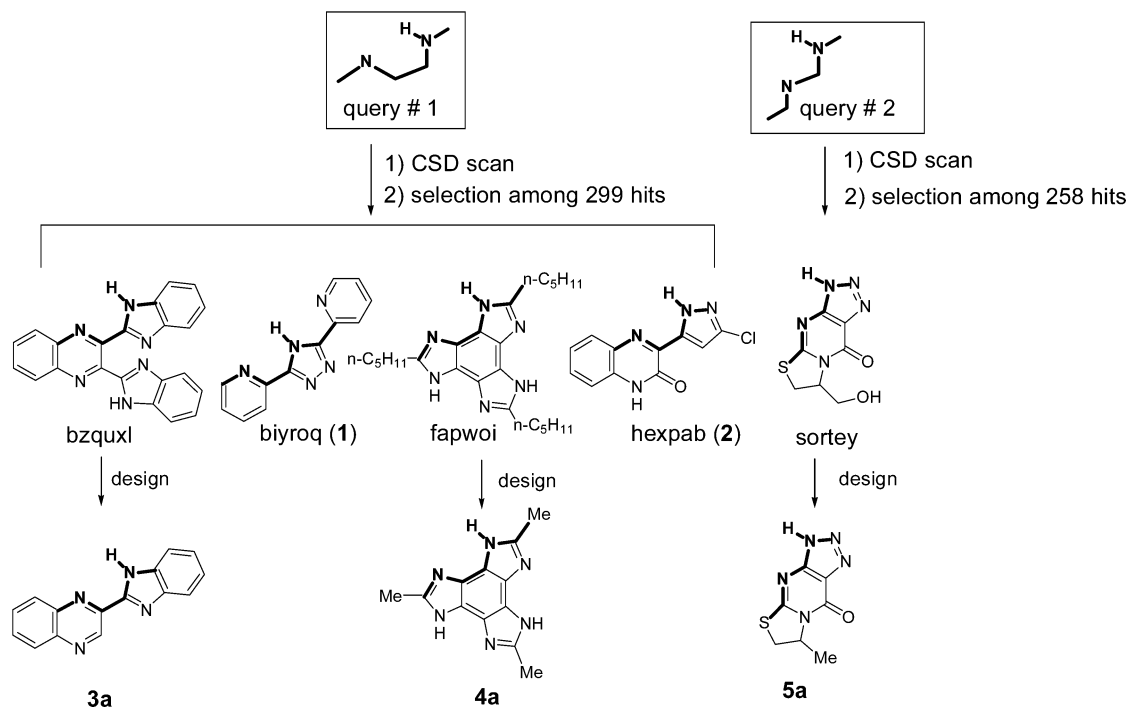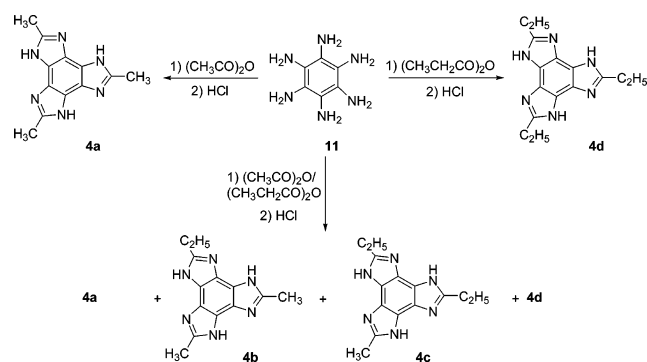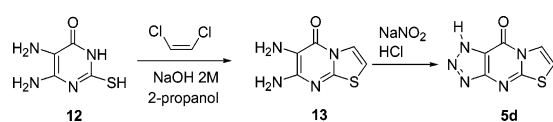
Figure 3. Structures and refcodes of the five hits identified by searching the CSD. Three out of the five hits (*bzquxl*, *fapwoi*, and *sortey*) were synthetically translated into analogues **3a**, **4a**, and **5a**, respectively, expected to display a higher affinity as antagonists at the A$_1$AR and/or the A$_3$AR.
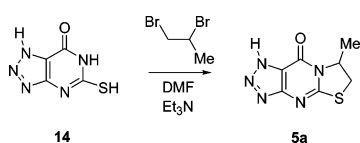
Scheme 4

Scheme 5

Scheme 6

1,2-dibromopropane to give a mixture of **5a** and the regioisomer in which the methyl group is on the C-2 atom. After column chromatography and recrystallization, compound **5a** was obtained with a 96% degree of purity.

Biology

The affinity of the new compounds toward human A$_1$, A$_{2A}$, and A$_3$ ARs was evaluated by competition experiments assessing their respective abilities to displace
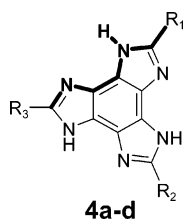
[³H]DPCPX, [³H]NECA, or [¹²⁵I]AB-MECA binding from transfected CHO cells. Experiments were performed as described elsewhere.[43]

Results and Discussion

Table 1 lists the binding affinities at the human A$_1$, A$_{2A}$, and A$_3$ ARs of compounds **1**, **2**, **3a**, **4a**, and **5a**, designed as antagonists of the A$_1$AR and/or the A$_3$AR as schematized in Figure 3. Although **1** did not elicit any appreciable affinity for any of the AR subtypes, the remaining compounds displayed submicromolar affinity at the A$_1$AR (**3a**) or the A$_3$AR (**2**, **4a**, and **5a**), consistent with our working hypothesis. The disappointing binding data of **1** might be ascribed to a combination of small molecular size and lipophilicity. Although the above drawbacks could have been solved by preparing alkyl derivatives of **1**, we decided to initially focus lead optimization efforts on the more promising and easily modifiable four active compounds **2**, **3a**, **4a**, and **5a**.

Three homologues of the 2,5,8-trimethylbenzotriimidazole **4a** were prepared and tested in an attempt to improve potency and retain selectivity at the A$_3$AR. As shown in Table 2, none of these compounds (**4b**−**d**) revealed a significant selectivity for either the A$_3$AR or the A$_1$AR. Incidentally, the triethyl derivative **4d** was slightly selective for the A$_1$AR.

The triazolopyrimidinone **5a** exhibited an interesting selectivity profile at the A$_3$AR (Table 3). Actually, this compound was assayed as a mixture made up of 96% of (*R,S*)-**5a** and 4% of the corresponding (*R,S*)-2-methyl isomer. However, in the context of our lead-finding strategy, there was no need to obtain **5a** with a higher purity level. Simple modifications about the thiazolidine ring of **5a** yielded compounds equipotent (**5c**) or inactive (**5b,d**) in the binding experiments. Research in this series is still in progress, and results will be reported in due time.

Table 2. Affinities at Human A_1, A_{2A}, and A_3 ARs of Compounds **4a−d**

4a-d

cmpd	R_1	R_2	R_3	K_i (nM)[a]		
				hA_1^b	hA_{2A}^c	hA_3^d
4a	CH_3	CH_3	CH_3	>10000	>10000	130 ± 3
4b	CH_3	CH_3	C_2H_5	496 ± 16	>10000	146.5 ± 21
4c	CH_3	C_2H_5	C_2H_5	966 ± 43	329 ± 18	135 ± 15
4d	C_2H_5	C_2H_5	C_2H_5	46 ± 4	720 ± 20	104.2 ± 9

[a] See footnote of Table 1 and K_i values of reference ligands. [b] See footnote of Table 1. [c] See footnote of Table 1. [d] See footnote of Table 1.

Table 3. Affinities at Human A_1, A_{2A}, and A_3 ARs of Compounds **5a−d**

5a   **5b**   **5c**   **5d**
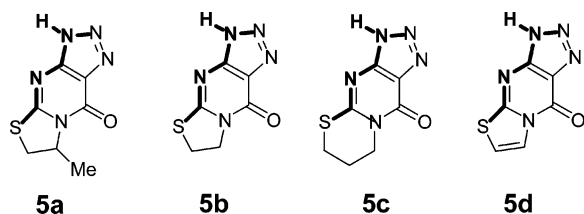
cmpd	K_i (nM)[a]		
	hA_1^b	hA_{2A}^c	hA_3^d
5a	>10000	>10000	440 ± 33
5b	>10000	>10000	>1000
5c	>10000	>10000	437 ± 51
5d	>10000	>10000	>1000

[a] See footnote of Table 1 and K_i values of reference ligands. [b] See footnote of Table 1. [c] See footnote of Table 1. [d] See footnote of Table 1.

Compounds **2** and **3a** were soon regarded as the most promising leads in the perspective of affinity and selectivity optimization at the target receptors (Table 1). Because **2** (fairly selective for the A_3AR) was a truncated analogue of **3a** (slightly selective for the A_1-AR), we hypothesized that 2-(benzimidazol-2-yl)quinoxaline (BIQ) would represent a suitable molecular scaffold to obtain both A_1AR and A_3AR selective antagonists. Several derivatives of **3a** were, in principle, obtainable from commercially available substituted-*o*-phenylendiamines, whereas structural modifications to compound **2** seemed more difficult and restricted to the replacement of the chlorine. Accordingly, we prepared and tested some BIQ derivatives substituted on the benzimidazole system (**3b−l**) or featuring isosteric CH → N variations about the benzimidazole ring (**3m−o**). Their structures and binding affinities at the A_1, A_{2A}, and A_3 ARs are summarized in Table 4. Compound **3e**, characterized by $R_1 = SC_2H_5$ in the benzimidazole 4′ position, stands out for its remarkable affinity and selectivity at the A_1AR (K_i values of 0.5, 3440, and 955 nM at the A_1AR, A_{2A}AR, and A_3AR, respectively). Interestingly, replacement of the SC_2H_5 of **3e** with the smaller and less lipophilic CH_3, to give **3b**, is associated with a 6000-fold drop in affinity at the A_1AR, as well as a 37-fold increase in potency at the A_3AR (K_i values

of **3b** are 8000, 833, and 26 nM at the A_1AR, A_{2A}AR, and A_3AR, respectively). The dramatic switch of selectivity observed on going from **3e** to **3b** is probably related to a better steric tolerance of the A_1AR cavity hosting the R_1 substituent/4′ position of the BIQ derivatives compared with that of the topologically analogous pocket of the A_3AR. Consistent with this hypothesis, **3d** and **3c** are increasingly less selective for the A_1AR over the A_3AR, owing to their less bulky R_1 substituents (SCH_3 and Cl, respectively). Replacement of the SC_2H_5 of **3e** with the relatively large NO_2 led to **3f** inactive at the A_1AR but provided appreciable affinity at the A_3AR. This fact apparently contradicts the above statement regarding the greater amount of room available to R_1 substituents at the A_1AR compared with that at the A_3AR. However, NO_2 is hydrophilic, whereas the groups so far considered in the same position (CH_3, Cl, SCH_3, and SC_2H_5) are lipophilic. Taken together, these data suggest that the A_1AR pocket hosting the R_1 substituent is mainly lipophilic. The poor binding profiles of the azaisosters **3m−o** can be reasonably ascribed to their unfavorable hydrophilicity.

A small substituent in the benzimidazole 5′ position (R_2), as in **3g−i**, is associated with little or no affinity at the ARs, thus suggesting that the corresponding binding sites (especially A_1AR and A_{2A}AR) do not have much room available for the R_2 substituent. The 5′ and 6′ positions bearing substituents R_2 and R_3 are chemically equivalent, thanks to the free rotation about the bond connecting the two heteroaromatic rings as well as tautomeric shifting of the imidazole hydrogen. The above-mentioned equivalence implies that steric encumbrance at the ARs should apply to both the 5′ and 6′ positions of the benzimidazole nucleus. Such a model explains the poor affinities of **3j** at the A_1AR and A_{2A}-AR and the substantial equipotence of **3j** and **3a** at the A_3AR. However, the high potency at the A_1AR of the 4′-methyl-6′-chloro derivative **3k** seems difficult to rationalize in the light of the structure−affinity relationships so far outlined. On comparing the K_i value of **3k** (3.6 nM) with the disappointing K_i values of **3b** and **3h** at the A_1AR, it becomes clear that the CH_3 and Cl substituents on the benzimidazole ring do not exert any additive effects on affinity. One can speculate that **3k** adopts a binding mode at the A_1AR different from those of the monosubstituted BIQ derivatives. Replacement of the CH_3 of **3k** with a Cl to give **3l** slightly increases the K_i values at the A_1AR and A_3AR, thus confirming that the electronic effects of R_1 and R_2 substituents do not play a significant role in tuning affinity at these receptors.

To sum up, a few chemically diverse antagonists at the human A_1AR and A_3AR were designed by a 3D searching of the CSD. Subsequent binding experiments confirmed the rationale of this design approach because four out the five tested compounds revealed appreciable affinities at one or both of the target receptors. Lead optimizations in the BIQ series **3** gave the best results in terms of potency and selectivity at the A_1AR as well as the A_3AR: **3e** exhibited K_i values at the A_1AR, A_{2A}-AR, and A_3AR of 0.5, 3440, and 955 nM, respectively, whereas **3b** displayed at the same ARs K_i values of 8000, 833, and 26 nM, respectively.

Table 4. Affinity of BIQs Derivatives **3a−o** at Human A₁, A₂ₐ, and A₃ ARs

					K_i (nM)[a]		
cmpd.	A	R₁	R₂	R₃	hA₁[b]	hA₂ₐ[c]	hA₃[d]
3a		H	H	H	50 ± 15	561 ± 17	763 ± 13
3b		CH₃	H	H	8000 ± 567	833 ± 67	26 ± 9
3c		Cl	H	H	350 ± 61	>10000	140 ± 20
3d		SCH₃	H	H	2.1 ± 0.3	3000 ± 200	278 ± 44
3e		SC₂H₅	H	H	0.5 ± 0.01	3440 ± 980	955 ± 215
3f		NO₂	H	H	>10000	>10000	879 ± 72
3g		H	CH₃	H	>10000	>10000	>1000
3h		H	Cl	H	>10000	>10000	632 ± 10
3i		H	OCH₃	H	>10000	>10000	>1000
3j		H	CH₃	CH₃	>10000	>10000	370 ± 35
3k		CH₃	H	Cl	3.6 ± 0.6	>10000	238 ± 32
3l		Cl	H	Cl	9.3 ± 1.2	>10000	699 ± 120
3m	[4,5-*b*]pyridine				>10000	>10000	>1000
3n	[4,5-*c*]pyridine				>10000	>10000	168 ± 23
3o	[4,5-*d*]pyrimidine				>10000	>10000	>1000

[a] See footnote of Table 1 and K_i values of reference ligands. [b] See footnote of Table 1. [c] See footnote of Table 1. [d] See footnote of Table 1.

Experimental Section

Chemistry. Melting points were determined using a Büchi apparatus B-540 and are uncorrected. Routine nuclear magnetic resonance spectra were recorded on a Varian Mercury 400 spectrometer operating at 400 MHz. EI and HRMS mass spectra were obtained on a Finnigan MAT95XP spectrometer using a direct injection probe and an electron beam energy of 70 eV. ESI mass spectra were recorded with a Micromass ZMD Waters Instrument or an Applied Biosystems API 2000. Evaporation was performed in vacuo (rotary evaporator). Analytical TLC was carried out on Merck 0.2 mm precoated silica gel aluminum sheets (60 F-254). Silica gel 60 (230−400 mesh) was used for column flash chromatography. Elemental analyses were performed by our Analytical Laboratory in Pisa and agreed with theoretical values to within ±0.4%.

3-Chloro-2-nitroaniline was commercially avalaible from Frinton Laboratories Inc., New Jersey, U.S.A.

General Procedure for the Synthesis of 2-(Substituted-*1H*-benzimidazol-2-yl)quinoxaline Derivatives 3a−l, 2-(1*H*-Imidazo[4,5-*b*]pyridin-2-yl)quinoxaline, 3m, 2-(1*H*-Imidazo[4,5-*c*]pyridin-2-yl)quinoxaline, 3n, and 2-(7*H*-Purin-8-yl)quinoxaline, 3o. A mixture of quinoxaline-2-carboxylic acid **6** (0.50 g, 2.9 mmol), the appropriate diamine **7a−o** (2.9 mmol), and polyphosphoric acid (17.5 g) was heated for 1 h at 125 °C and then for 2 h at 200 °C. The mixture was poured into a large volume of ice−water, and the solid mass was collected. The crude product was treated with saturated sodium bicarbonate solution and purified by chromatography to give the desired derivative **3a−o**. Yields, melting points, and analytical and spectral data are reported in the Supporting Information.

General Procedure for the Synthesis of 2,5,8-Trimethyl-4,7-dihydro-*1H*-benzo[1,2-*d*:3,4-*d′*:5,6-*d″*]triimidazole, 4a, and 2,5,8-Triethyl-4,7-dihydro-*1H*-benzo[1,2-*d*:3,4-*d′*:5,6-*d″*]triimidazole, 4d. A solution of benzenehexamine **11** (0.50 g, 2.91 mmol) and the appropriate anhydride (15 mL) was stirred under a nitrogen atmosphere at 170 °C until a white precipitate formed (1.5 h). The solid was taken off by filtration, and the filtrate was refluxed with HCl 4 N (15 mL) for 4 h under a nitrogen atmosphere. The solution was made alkaline with NaOH 2 N, and the precipitated solid was collected and purified by flash chromatography (CHCl₃−CH₃-OH, 9:1 v/v as the eluant) and then recrystallized from ethyl

acetate. Yields, melting points, and analytical and spectral data are reported in the Supporting Information.

General Procedure for the Synthesis of 2-Ethyl-5,8-dimethyl-4,7-dihydro-*1H*-benzo[1,2-*d*:3,4-*d′*:5,6-*d″*]triimidazole, 4b, and 2,5-Diethyl-8-methyl-4,7-dihydro-*1H*-benzo[1,2-*d*:3,4-*d′*:5,6-*d″*]triimidazole, 4c. Following the above-reported procedure, benzenehexamine **11** (0.50 g, 2.91 mmol) was reacted with a mixture of acetic anhydride (5 mL) and propionic anhydride (10 mL). The precipitated solid, containing the derivatives **4a−d**, was flash chromatographed (CHCl₃−CH₃OH, 9:1 v/v as the eluant) to separate the four components. The fastest running band was identified as **4d** (traces), the second band was the derivative **4c** (10%), then **4b** (12%), and the slowest band was **4a** (15%). Each compound was recrystallized from ethyl acetate. Melting points and analytical and spectral data are reported in the Supporting Information.

7-Methyl-6,7-dihydro[1,3]thiazolo[3,2-*a*][1,2,3]triazolo-[4,5-*d*]pyrimidin-9(1*H*)-one, 5a. 1,2-Dibromopropane (0.62 mL, 6.0 mmol) and triethylamine (0.92 mL, 6.6 mmol) were slowly added to a stirred suspension of **14**[42] (1.02 g, 6.0 mmol) in anhydrous DMF (8 mL), and then the mixture was heated at reflux for 1 h. After cooling and concentration to dryness, the residue obtained, made up of a mixture of 6-methyl and 7-methyl isomers (¹H NMR spectrum), was flash chromatographed (CHCl₃−MeOH, 9:1 v/v as the eluant). After recrystallization from water, the 7-methyl isomer **5a** was obtained with a 96% degree of purity and a yield of 17%. ¹H NMR (DMSO-*d₆*): δ 16.06 (bs exch, 1H, NH), 5.15 (m, 1H, CH), 3.98 (m, 1H, CH₂), 3.24 (m, 1H, CH₂), 1.38 (d, 3H, CH₃). MS (EI) *m/z* (%): 209 (M⁺, 100); 194 (35); 181 (25); 165 (22); 148 (10); 126 (6); 111 (27); 86 (33). HRMS: 209.01160, C₇H₇N₅OS requires 209.03713.

[1,3]Thiazolo[3,2-*a*][1,2,3]triazolo[4,5-*d*]pyrimidin-9(1*H*)-one, 5d. Crystalline sodium nitrite (0.22 g, 3.2 mmol) was slowly added to a stirred suspension of **13** (0.5 g, 2.7 mmol) in 20 mL of HCl 6 M in an ice bath. After the addition was complete, the solution was left to stand at room temperature for 4 h, heated at 50 °C for 40 min, and then concentrated to half volume and cooled. The resulting precipitate consisted of pure **5d** (80%). Mp 265−266 °C. ¹H NMR (DMSO-*d₆*): δ 11.24 (bs exch, 1H, NH), 8.08 (d, 1H, H-3), 7.42 (d, 1H, H-2). MS

(EI) m/z (%): 193 (M⁺, 100); 165 (6); 110 (51). HRMS: 193.03520, $C_6H_3N_5OS$ requires 193.00583.

General Procedure for the Synthesis of 3-(Methylthio)benzene-1,2-diamine, 7d, and 3-(Ethylthio)benzene-1,2-diamine, 7e. A solution of 3-(methylthio)-2-nitroaniline (**10d**)[39] or 3-(ethylthio)-2-nitroaniline (**10e**) (3.3 mmol) and tin-(II)chloride dihydrate (3.72 g, 16.5 mmol) in ethyl acetate (30 mL) was heated at reflux for 2 h. After cooling, the reaction mixture was diluted with 70 mL of ethyl acetate and poured into ice−water (200 mL). While stirring, the pH was adjusted to 8 with saturated sodium bicarbonate solution, and the precipitate that formed was filtered off. The aqueous phase was separated and extracted three times with 50 mL portions of ethyl acetate. The combined organic phases were dried (Na_2SO_4) and evaporated to dryness to give the desired compounds **7d** (86%) or **7e** (92%), respectively. These compounds were employed without further purification.

7d: ¹H NMR (CDCl₃): δ 6.96−6.93 (m, 1H, H-Ar), 6.69−6.64 (m, 2H, H-Ar), 4.35−3.23 (bs, 4H, 2 × NH₂), 2.36 (s, 3H, CH₃). ESI (CH₃OH): 178.8 [M + Na⁺].

7e: ¹H NMR (CDCl₃): 6.98−6.94 (m, 1H, H-Ar), 6.75−6.64 (m, 2H, H-Ar), 4.25−3.21 (bs, 4H, 2 × NH₂), 2.75 (q, 2H, CH₂), 1.22 (t, 3H, CH₃). ESI (CH₃OH): 191.6 [M + Na⁺].

3-(Ethylthio)-2-nitroaniline, 10e. A solution of NaSEt (0.58 g, 6.9 mmol) in DMF (7 mL) was added dropwise to a stirred solution of 3-chloro-2-nitroaniline (**9**) (1.0 g, 5.8 mmol) in DMF (25 mL) at 20 °C. After the addition was complete, the mixture was stirred for 1 h at 40 °C and refluxed for 2 h. The solvent was evaporated to dryness, and the residue was chromatographed (ethyl acetate−n-hexane, 7:3 v/v as the eluant) to give **10e** (30%). ¹H NMR (CDCl₃): δ 7.16 (t, 1H, H-5), 6.60 (d, 1H, H-4), 6.54 (d, 1H, H-6), 5.80 (bs, 2H, NH₂), 2.89 (q, 2H, CH₂), 1.34 (t, 3H, CH₃).

6,7-Diamino-5H-[1,3]thiazolo[3,2-a]pyrimidin-5-one, 13. Propan-2-ol (32 mL) was added to a solution of NaOH 2 M (32 mL) containing 4,5-diamino-6-hydroxy-2-mercaptopyrimidine (**12**) (5.0 g, 31 mmol). A light precipitate was immediately formed. *cis*-1,2-Dichloroethene (2.49 mL, 33 mmol) was then slowly added to the reaction mixture at room temperature, and stirring was continued at the same temperature for 2 h and then at 60−70 °C for a further 5 h. After cooling, the solvents were removed, and the residue was treated with H_2O (20 mL) and exhaustively extracted with ethyl acetate. The organic extracts were dried over Na_2SO_4 and then evaporated to dryness to yield a solid that was purified by flash-chromatography (CH_2Cl_2−MeOH, 9:1 v/v as the eluant) to give **13** (10%). Mp 170−172 °C. ¹H NMR (DMSO-d_6): δ 7.76 (d, 1H, J = 5.0 Hz, H-3), 7.20 (d, 1H, J = 5.0 Hz, H-2), 6.12 (s, 2H, 7-NH₂), 3.64 (s, 2H, 6-NH₂).

Biological Methods. Materials. [³H]DPCPX, [³H] NECA, and [¹²⁵I]AB-MECA were obtained from DuPont-NEN (Boston, MA). Adenosine deaminase (ADA) was from Sigma Chemical Co. (St. Louis, MO). All other reagents were from standard commercial sources and of the highest commercially available grade.

Adenosine Receptor Binding Assay. Human A₁ Adenosine Receptors. Aliquots of membranes (50 μg proteins) obtained from A₁ CHO cells were incubated at 25 °C for 180 min in 500 μL of T_{1b}/T_{1h} buffer (50 mM Tris−HCl, 2 mM MgCl₂, pH 7.7)/(50 mM Tris−HCl, 2 mM MgCl₂, 2 units/mL ADA, pH 7.4) containing [³H]DPCPX (3 nM) and six different concentrations of the newly synthesized compounds. Nonspecific binding was determined in the presence of 50 μM RPIA.

The dissociation constant (K_d) of [³H]DPCPX A₁ CHO cell membranes was 3 nM.

Human A₂A Adenosine Receptors. Aliquots of cell membranes (80 μg) were incubated at 25 °C for 90 min in 500 μL of T_{2h} buffer (50 mM Tris−HCl, 2 mM MgCl₂, 2 units/mL ADA, pH 7.4) in the presence of 30 nM of [³H]NECA and six different concentrations of the newly synthesized compounds. Nonspecific binding was determined in the presence of 100 μM NECA. The dissociation constant (K_d) of [³H]NECA in A₂A CHO cell membranes was 30 nM.

Human A₃ Adenosine Receptors. Aliquots of cell membranes (40 μg) were incubated at 25 °C for 90 min in 100 μL of T_{3h} buffer (50 mM Tris−HCl, 10 mM MgCl₂, 1 mM EDTA, 2 units/mL ADA, pH 7.4) in the presence of 1.4 nM [¹²⁵I]AB-MECA and six different concentrations of the newly synthesized compounds. Nonspecific binding was determined in the presence of 50 μM RPIA. The dissociation constant (K_d) of [¹²⁵I] AB-MECA in A₃ CHO cell membranes was 1.4 nM.

All compounds were routinely dissolved in DMSO and diluted with assay buffer to the final concentration, where the amount of DMSO never exceeded 2%. Percentage inhibition values of specific radiolabeled ligand binding at 1−10 μM concentration are means ± SEM of at least three determinations. At least six different concentrations spanning 3 orders of magnitude, adjusted appropriately for the IC₅₀ of each compound, were used. IC₅₀ values, computer-generated using a nonlinear regression formula on a computer program (Graph-Pad, San Diego, CA), were converted to K_i values, knowing the K_d values of radioligands in the different tissues and using the Cheng and Prusoff equation.[44] K_i values are means ± SEM of at least three determinations.

Supporting Information Available: Physical and spectral data of **3** and **4** and analytical data of **3**−**5**. This material is available free of charge via the Internet at http://pubs.acs.org.

References

(1) Wardas, J. Neuroprotective Role of Adenosine in the CNS. *Pol. J. Pharmacol.* **2002**, *54*, 313−326.

(2) Ribeiro, J. A.; Sebastião, A. M.; de Mendonça, A. Adenosine Receptors in the Nervous System: Pathophysiological Implications. *Prog. Neurobiol. (Amsterdam, Neth.)* **2003**, *68*, 377−392.

(3) Poulsen, S.-A.; Quinn, R. J. Adenosine Receptors: New Opportunities for Future Drugs. *Bioorg. Med. Chem.* **1998**, *6*, 619−641.

(4) Rorke, S.; Holgate, S. T. Targeting Adenosine Receptors: Novel Therapeutic Targets in Asthma and Chronic Obstructive Pulmonary Disease. *Am. J. Respir. Med.* **2002**, *1*, 99−105.

(5) Nishiyama, A.; Rahman, M.; Inscho, E. W. Role of Interstitial ATP and Adenosine in the Regulation of Renal Hemodynamics and Microvascular Function. *Hypertens. Res.* **2004**, *27*, 791−804.

(6) Fredholm, B. B.; IJzerman, A. P.; Jacobson, K. A.; Klotz, K.-N.; Linden, J. International Union of Pharmacology. XXV. Nomenclature and Classification of Adenosine Receptors. *Pharmacol. Rev.* **2001**, *53*, 527−552.

(7) Dhalla, A. K.; Shryock, J. C.; Shreeniwas, R.; Belardinelli, L. Pharmacology and Therapeutic Applications of A₁ Adenosine Receptor Ligands. *Curr. Top. Med. Chem.* **2003**, *3*, 369−385.

(8) Ferre, S.; Fredholm, B. B.; Morelli, M.; Popoli, P.; Fuxe, K. Adenosine−Dopamine Receptor−Receptor Interactions as an Integrative Mechanism in the Basal Ganglia. *Trends Neurosci.* **1997**, *20*, 482−487.

(9) Franco, R.; Ferre, S.; Agnati, L.; Torvinen, M.; Gines, S.; Hillion, J.; Casado, V.; Lledo, P.; Zoli, M.; Lluis, C.; Fuxe, K. Evidence for Adenosine/Dopamine Receptor Interactions: Indications for Heteromerization. *Neuropsychopharmacology* **2000**, *23*, S50−59.

(10) Fink, J. S.; Weaver, D. R.; Rivkees, S. A.; Peterfreund, R. A.; Pollack, A. E.; Adler, E. M.; Reppert, S. M. Molecular Cloning of the Rat A₂ Adenosine Receptor: Selective co-Expression with D₂ Dopamine Receptors in Rat Striatum. *Mol. Brain Res.* **1992**, *14*, 186−195.

(11) Cacciari, B.; Pastorin, G.; Spalluto, G. Medicinal Chemistry of A₂A Adenosine Receptor Antagonists. *Curr. Top. Med. Chem.* **2003**, *3*, 403−411.

(12) Fredholm, B. B.; Cuhna, R. A.; Svenningsson, P. Pharmacology of Adenosine A₂A Receptors and Therapeutic Applications. *Curr. Top. Med. Chem.* **2003**, *3*, 413−426.

(13) Linden, J. Cloned Adenosine A₃ Receptors: Pharmacological Properties, Species Differences and Receptor Functions. *Trends Pharmacol. Sci.* **1994**, *15*, 298−306.

(14) Jacobson, K. A.; Kim, H. O.; Siddiqui, S. M.; Olah, M. E.; Stiles, G. L.; Von Lubitz, D. K. J. E. A₃-Adenosine Receptors: Design of Selective Ligands and Therapeutic Prospects. *Drugs Future* **1995**, *20*, 689−701.

(15) Müller, C. E. Medicinal Chemistry of Adenosine A₃ Receptor Ligands. *Curr. Top. Med. Chem.* **2003**, *3*, 445−462.

(16) Fishman, P.; Bar-Yehuda, S. Pharmacology and Therapeutic Applications of A₃ Receptor Subtypes. *Curr. Top. Med. Chem.* **2003**, *3*, 463−469.

(17) Martin, Y. C. 3D Database Searching in Drug Design. *J. Med. Chem.* **1992**, *35*, 2145−2154.

(18) Lipinski, C. A.; Lombardo, F.; Dominy, B. W.; Feeney, P. J. Experimental and Computational Approaches to Estimate Solubility and Permeability in Drug Discovery and Developing Settings. *Adv. Drug Delivery Rev.* **1997**, *23*, 3−25.

(19) Guandalini, L.; Martini, E.; Dei, S.; Manetti, D.; Scapecchi, S.; Teodori, E.; Romanelli, M. N.; Varani, K.; Greco, G.; Spadola, L.; Novellino, E. Design of Novel Nicotinic Ligands through 3D Database Searching. *Bioorg. Med. Chem.* **2005**, *13*, 799−807.

(20) Enyedy, I. J.; Sakamuri, S.; Zaman, W. A.; Johnson, K. M.; Wang, S. Pharmacophore-Based Discovery of Substituted Pyridines as Novel Dopamine Transporter Inhibitors. *Bioorg. Med. Chem. Lett.* **2003**, *13*, 513−517.

(21) Chen, G. S.; Chang, C.-S.; Kan, W. M.; Chang, C.-L.; Wang, K. C.; Chern, J.-W. Novel Lead Generation through Hypothetical Pharmacophore Three-Dimensional Database Searching: Discovery of Isoflavonoids as Nonsteroidal Inhibitors of Rat 5α-Reductase. *J. Med. Chem.* **2001**, *44*, 3759−3763.

(22) Zaharevitz, D. W.; Gussio, R.; Wiegand, A.; Jalluri, R.; Pattabiraman, N.; Kellogg, G. E.; Pallansch, L. A.; Yang, S. S.; Buckheit, R. W., Jr. Discovery of Novel HIV-1 Reverse Transcriptase Inhibitors Using a Combination of 3D Database Searching and 3D QSAR. *J. Med. Chem.* **1999**, *9*, 551−564.

(23) Marriott, D. P.; Dougall, I. G.; Meghani, P.; Liu, Y.-J.; Flower, D. R. Lead Generation Using Pharmacophore Mapping and Three-Dimensional Database Searching: Application to Muscarinic M₃ Receptor Antagonists. *J. Med. Chem.* **1999**, *42*, 3210−3216.

(24) Wang, S.; Zaharevitz, D. W.; Sharma, R.; Marquez, V. E.; Lewin, N. E.; Du, L.; Blumberg, P. M.; Milne, G. W. The Discovery of Novel, Structurally Diverse Protein Kinase C Agonists through Computer 3D-Database Pharmacophore Search. Molecular Modeling Studies. *J. Med. Chem.* **1994**, *37*, 4479−4489.

(25) Allen, F. H.; Bellard, S.; Brice, M. D.; Cartwright, B. A.; Doubleday, A.; Higgs, H.; Hummelink, T.; Hummelink-Peters, B. G.; Kennard, O.; Motherwell, W. D. S.; Rodgers, J. R.; Watson, D. G. The Cambridge Crystallographic Data Centre: Computer-Based Search, Retrieval, Analysis and Display of Information. *Acta Crystallogr., Sect. B: Struct. Sci.* **1979**, *35*, 2231−2239.

(26) Suzuki, F.; Shimada, J.; Shiozaki, S.; Ichikawa, S.; Ishii, A.; Nakamura, J.; Nonaka, H.; Kobayashi, H.; Fuse, E. Adenosine A₁ Antagonists. 3. Structure−Activity Relationships on Amelioration against Scopolamine- or N^6-((R)-Phenylisopropyl)adenosine-Induced Cognitive Disturbance. *J. Med. Chem.* **1993**, *36*, 2508−2518.

(27) van Galen, P. J. M.; Nissen, P.; van Wijngaarden, I.; IJzerman, A. P.; Soudijn, W. 1H-Imidazo[4,5-c]quinolin-4-amines: Novel Non-Xanthine Adenosine Antagonists. *J. Med. Chem.* **1991**, *34*, 1202−1206.

(28) Saki, M.; Tsumuki, H.; Nonaka, H.; Shimada, J.; Ichimura, M. KF26777 (2-(4-Bromophenyl)-7,8-dihydro-4-propyl-1H-imidazo-[2,1-i]purin-5(4H)-one), a New Potent and Selective Adenosine A₃ Receptor Antagonist. *Eur. J. Pharmacol.* **2002**, *444*, 133−141.

(29) Francis, J. E.; Cash, W. D.; Psychoyos, S.; Ghai, G.; Wenk, P.; Friedmann, R. C.; Atkins, C.; Warren, V.; Furness, P.; Hyun, J. L.; Stone, G. A.; Desai, M.; Williams, M. Structure−Activity Profile of a Series of Novel Triazoloquinazoline Adenosine Antagonists. *J. Med. Chem.* **1988**, *31*, 1014−1020.

(30) Baraldi, P. G.; Cacciari, B.; Moro, S.; Spalluto, G.; Pastorin, G.; Da Ros, T.; Klotz, K.-N.; Varani, K.; Gessi, S.; Borea, P. A. Synthesis, Biological Activity, and Molecular Modeling Investigation of New Pyrazolo[4,3-e]-1,2,4-triazolo[1,5-c]pyrimidine Derivatives as Human A₃ Adenosine Receptor Antagonists. *J. Med. Chem.* **2002**, *45*, 770−780.

(31) van Muijlwijk-Koezen, J. E.; Timmerman, H.; van der Goot, H.; Menge, W. M. P. B.; Frijtag von Drabbe Kunzel, J.; de Groote, M.; IJzerman, A. P. Isoquinoline and Quinazoline Urea Analogues as Antagonists for the Human Adenosine A₃ Receptors. *J. Med. Chem.* **2000**, *43*, 2227−2238.

(32) Bruno, I. J.; Cole, J. C.; Edgington, P. R.; Kessler, M.; Macrae, C. F.; McCabe, P.; Pearson, J.; Taylor, R. New Software for Searching the Cambridge Structural Database and Visualizing Crystal Structures. *Acta Crystallogr., Sect. B: Struct. Sci.* **2000**, *58*, 389−397.

(33) Kanoktanaporn, S.; MacBride, J. A. H.; King, T. J. Displacement of Hydrazine Hydrochloride from 1,4-Dichlorophthalazines by Bidentate Nucleophiles with Formation of 2,2′-(1,2-Arylene)bis-Benzimidazoles and -Benzothiazoles. X-ray Crystal Structure of 2,3-Bisbenzimidazol-2-ylquinoxaline. *J. Chem. Res., Synop.* **1980**, *12*, 406.

(34) Prins, R.; Birker, P. J. M. L.; Verschoor, G. C. Structure of 2-[5-(2-Pyridyl)-1H-1,2,4-triazol-3-yl]pyridinium Perchlorate *Acta Crystallogr., Sect. B: Struct. Sci.* **1982**, *38*, 2934−2935.

(35) Kohne, B.; Praefcke, K.; Derz, T.; Gondro, T.; Frolow, F. Benzenetris(imidazole). A New Ring System from Benzenehexamine. *Angew. Chem., Int. Ed. Engl.* **1986**, *25*, 650−651.

(36) Heinisch, G.; Matuszczak, B.; Mereiter, K. Pyridazines. 71. A Novel Type of 1,2-Diazine by Ring Contraction of 1,2-Diazole. *Heterocycles* **1994**, *38*, 2081−2089.

(37) Pecorari, P.; Rinaldi, M.; Costi, M. P.; Antolini, L. Cyclization Reactions of 1,3-Dibromopropan-2-ol, 2,3-Dibromopropan-1-ol and 1-Bromomethyloxirane with 6-Amino-2,3-dihydro-2-thioxo-4(1H)-pyrimidinone. *J. Heterocycl. Chem.* **1991**, *28*, 891−898.

(38) Mizutani, T.; Yoshida, K.; Kawazoe, S. Formation of Toxic Metabolites from Thiabendazole and Other Thiazoles in Mice. Identification of Thioamides as Ring Cleavage Products. *Drug Metab. Dispos.* **1994**, *22*, 750−755.

(39) Hay, M. P.; Gamage, S. A.; Kovacs, M. S.; Prujin, F. B.; Anderson, R. F.; Patterson, A. V.; Wilson, W. R.; Brown, J. M.; Denny, W. A. Structure−Activity Relationships of 1,2,4-Benzotriazine 1,4-Dioxides as Hypoxia-Selective Analogues of Tirapazamine. *J. Med. Chem.* **2003**, *46*, 169−182.

(40) Wolff, J. J.; Limbach, H.-H. Synthesis and Spectroscopic Characterization of ¹⁵N-Labeled Hexaaminobenzene Derivatives. *Liebigs Ann. Chem.* **1991**, 691−693.

(41) Pecorari, P.; Rinaldi, M.; Costi, M. P. New Heterocyclic Structures. [1,3]Thiazino[3,2-a]purine and [1,2,3]Triazolo[4,5-d][1,3]-thiazino[3,2-a]pyrimidine. *J. Heterocycl. Chem.* **1989**, *26*, 1701−1705.

(42) Bahner, C. T.; Bilancio, D. E. 5-Thiol-7-hydroxy-1-γ-triazolo[d]-pyrimidine, *J. Am. Chem. Soc.* **1953**, *75*, 6038.

(43) Da Settimo, F.; Primofiore, G.; Taliani, S.; La Motta, C.; Novellino, E.; Greco, G.; Lavecchia, A.; Cosimelli, B.; Iadanza, M.; Klotz, K.-N.; Tuscano, D.; Trincavelli, M. L.; Martini, C. A₁ Adenosine receptor Antagonists, 3-Aryl[1,2,4]triazinobenzimidazol-4-(10H)-ones (ATBIs) and N-alkyl and N-acyl-(7-substituted-2-phenylimidazo[1,2-a][1,3,5]triazin-4-yl)amines (ITAs): Different Recognition of Bovine and Human Binding Sites. *Drug Dev. Res.* **2004**, *63*, 1−7.

(44) Cheng, Y. C.; Prusoff, W. H. Relationship between the Inhibition constant (K_i) and the Concentration of Inhibitor which causes 50% Inhibition (IC_{50}) of an Enzymatic Reaction. *Biochem. Pharmacol.* **1973**, *22*, 3099−3108.